



Cite this: *Org. Biomol. Chem.*, 2018, **16**, 1144

## Synthesis of a novel HER2 targeted aza-BODIPY–antibody conjugate: synthesis, photophysical characterisation and *in vitro* evaluation†

Miffy. H. Y. Cheng,<sup>a</sup> Antoine Maruani,<sup>b</sup>  Huguette Savoie,<sup>a</sup> Vijay Chudasama \*<sup>b</sup> and Ross. W. Boyle \*<sup>a</sup>

Received 30th November 2017,  
Accepted 16th January 2018

DOI: 10.1039/c7ob02957h

rsc.li/obc

We herein report the synthesis and analysis of a novel aza-BODIPY–antibody conjugate, formed by controlled and regioselective bioconjugation methodology. Employing the clinically relevant antibody, which targets HER2 positive cancers, represents an excellent example of an antibody targeting strategy for this class of near-IR emitting fluorophore. The NIR fluorescence and binding properties were validated through *in vitro* studies using live cell confocal imaging.

### Introduction

Near infrared (NIR) fluorescence imaging has attracted much attention over the last decade due to its advantageous properties compared to visible region fluorescence. These include deeper tissue penetration for *in vivo* applications, reduced autofluorescence and minimisation of light scattering, leading to improved signal-to-noise ratios.<sup>1</sup> This is of particular interest in fluorescence guided surgery (FGS), as the technique can provide a stronger contrast between healthy and neoplastic tissues, therefore generally improving surgical accuracy.<sup>2</sup> Breast conserving surgery is an example that can benefit from FGS, as precise identification of the tumours is essential for tissue preservation and preventing incomplete resection.<sup>3</sup> However, many of the current FDA-approved NIR emitting fluorophores suffer from inaccurate targeting and poor photostability, thus limiting their application for NIR FGS. Despite many efforts to produce targeted NIR emitting fluorophores, poor photophysical properties or solubility issues limit their use in biological imaging.<sup>4</sup> Therefore, there is a high demand for the development of this class of imaging agents with improved physicochemical properties.<sup>5</sup>

The aza-borondipyrromethenes (BODIPYs) are a relatively new class of NIR emitting fluorophores with excellent photostability and promising photophysical profile for FGS. Due to their outstanding properties, this class of compounds have

recently been the subject of many biological studies<sup>6–10</sup> and material based applications.<sup>11–13</sup> In spite of this growing interest, the use of these scaffolds in bioconjugation and targeted imaging applications has remained limited.<sup>14</sup> This is primarily due to the synthetic challenges in introducing conjugation moieties<sup>15,16</sup> as well as solubility issues associated with structural modifications.<sup>17</sup> Hence, successful preparation of antibody–aza-BODIPY-based conjugates has hitherto not been achieved.

Since many tumours have been shown to overexpress receptors, both specificity and selectivity can be significantly improved by targeting NIR emitting probes to these biomarkers, offering the possibility of better contrast and detection of tumours. Monoclonal antibodies have been used extensively as targeting moieties in biological and clinical research to enhance affinity of drugs and imaging agents towards overexpressed receptors in cancerous tissues;<sup>18,19</sup> they can be covalently bound to fluorescent probes to obtain fluorescent antibody conjugates (FAC) for use in fluorescence imaging. Several FACs are in preclinical development featuring both FDA-approved antibodies and commercially available fluorophores.<sup>20–23</sup> However, FACs are most commonly generated through multiple lysine labelling and this methodology results in heterogeneous mixtures of products that suffer from variability between batches.<sup>24</sup> Therefore, this could affect selectivity and specificity for target tissue, resulting in poor imaging in FGS. To alleviate these issues, site selective bioconjugation methods have been developed. A promising approach was recently introduced by Chudasama and co-workers<sup>25,26</sup> with the use of dibromopyridazinediones (PDs) to regioselectively modify cysteine residues through disulfide rebridging and the applicability of this method has been demonstrated in a variety of antibody conjugates.<sup>26–30</sup>

<sup>a</sup>University of Hull, Department of Chemistry, Cottingham Road, Hull, HU6 7RX, United Kingdom of Great Britain and Northern Ireland. E-mail: r.w.boyle@hull.ac.uk

<sup>b</sup>University College London, Department of Chemistry, 20 Gordon Street, London, WC1H 0AJ, United Kingdom of Great Britain and Northern Ireland

† Electronic supplementary information (ESI) available. See DOI: 10.1039/c7ob02957h



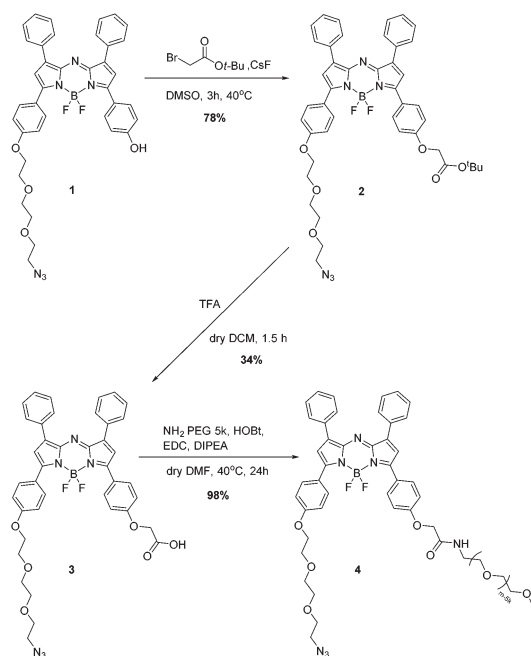
Herein, we report the synthesis and analysis of a water soluble aza-BODIPY and its regioselective conjugation to trastuzumab, a clinically relevant monoclonal antibody, in a controlled and efficient method using strained alkyne-functionalised dibromopyridazinedione in a copper-free strain-promoted alkyne-azide cycloaddition (SPAAC) reaction with water soluble azido aza-BODIPY, and subsequent *in vitro* validations of the resulting conjugate.

## Results and discussion

### Synthesis and characterisation

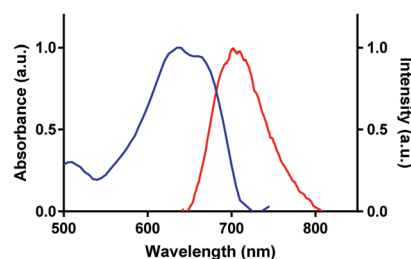
Firstly, we explored the synthesis of an azido aza-BODIPY with enhanced water solubility, which was compatible with the bioconjugation strategy described above. Azide-functionalised aza-BODIPY **1** was synthesised by adapting a method previously reported by our group.<sup>31</sup> It was then further modified as shown in Scheme 1.

Briefly, S<sub>N</sub>2 Williamson ether synthesis was performed at the available phenolate to introduce a protected ester, in a 78% yield. Deprotection of the *t*-butyl group was achieved using TFA, the reaction was carefully monitored to circumvent removal of BF<sub>2</sub> under acidic conditions, and deprotection was found to be complete after 1.5 h, following purification the carboxylic acid **3** was obtained in 34% yield. To enhance water solubility, an amine substituted 5 kDa-PEG chain was reacted with the corresponding carboxylic acid **3** through amide coupling in dry DMF at 40 °C for 24 h. The crude was purified using a C18 cartridge to obtain the water soluble aza-BODIPY **4** in 98% yield (Scheme 1).



Scheme 1 Synthesis of water soluble azido aza-BODIPY.

### Normalised UV-vis and fluorescence spectra of **4** in water



### Photostability evaluation of **4** against ICG

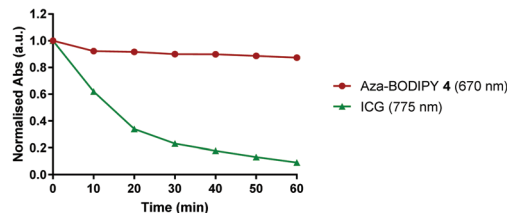


Fig. 1 Normalised absorption and emission spectra of **4** in water  $\lambda_{\text{abs}}$  (blue) and  $\lambda_{\text{em}}$  (red). Photostability study for **4** and ICG in PBS (pH 7.4).

### Photophysical studies

Photophysical evaluation of the aza-BODIPY **4** in aqueous media was carried out and showed absorption and emission maxima in water at 635 nm and 713 nm respectively. The compound was shown to exhibit excellent photostability from the photobleaching study through continuous illumination (>600 nm) for 60 minutes at 10  $\mu\text{M}$  in PBS (pH 7.4), a decrease of 13% of the absorbance was observed for **4**; however, this compared favourably with the commonly used NIR emitting fluorophore indocyanine green (ICG), which showed a 90% decrease under the same conditions after 60 minutes (Fig. 1).

In addition, the fluorescence quantum yield of aza-BODIPY **4** was calculated, and was found to be 0.19, this showed slightly lower fluorescence quantum yield in comparison to literature values, but acceptable as a NIR fluorescence probe (ESI<sup>†</sup>).

### Bioconjugation

Following on from the successful synthesis and promising properties of aza-BODIPY **4**, we set about synthesising a “clickable” antibody that would enable the controlled and site-selective attachment of the imaging moiety. We have recently shown that the functional rebridging of trastuzumab disulfide bonds using pyridazinedione derivative **5** enabled the preparation of a stable and modular platform, **7**, that can be functionalised in a rapid and facile manner (Fig. 2 and Scheme 2).<sup>26</sup> The presence of a highly and orthogonally reactive strained alkyne moiety makes this versatile bioconjugate amenable to copper-free strain-promoted alkyne-azide cycloaddition (SPAAC) reaction with a variety of substrates.

Following preparation of conjugate **7**, it was reacted with aza-BODIPY **4** using SPAAC chemistry (Scheme 3). After optimisation of the conditions, it was found that incubation of conjugate **7** with 6 equivalents (*i.e.* 1.5 eq. per strained alkyne) of



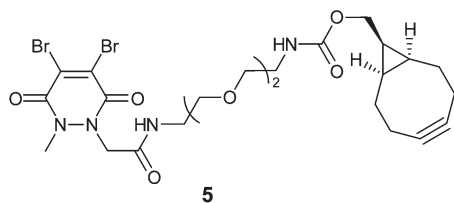
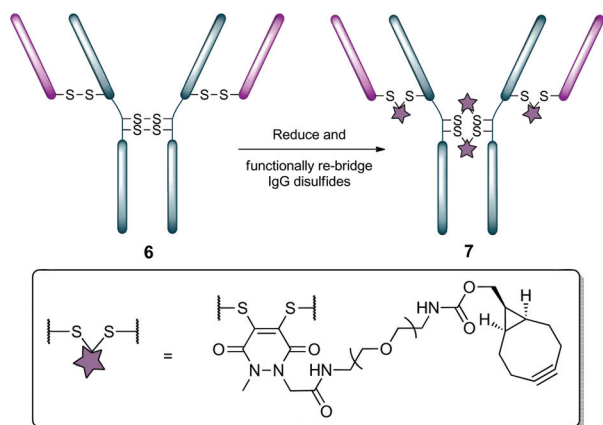
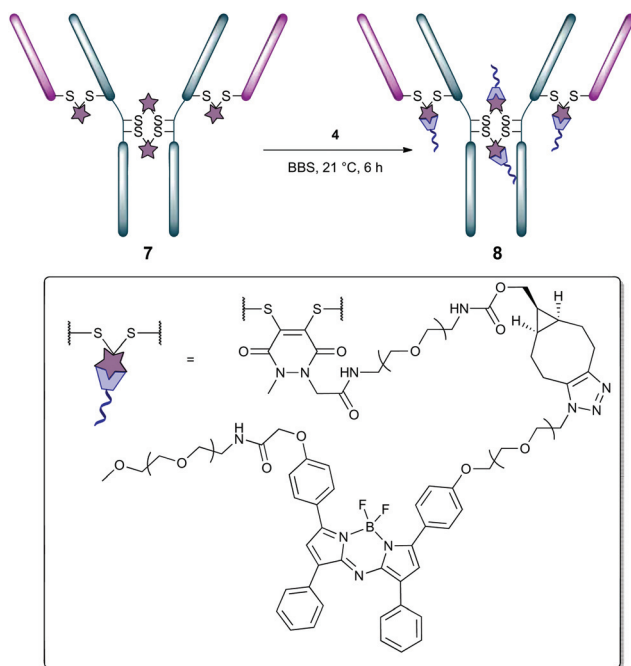


Fig. 2 Structure of PD-based re-bridging reagent.



Scheme 2 Preparation of "clickable" trastuzumab 7.



Scheme 3 Preparation of aza-BODIPY-trastuzumab conjugate 8.

aza-BODIPY 4 for 6 h at 21 °C, was sufficient to effect complete conversion to aza-BODIPY-trastuzumab conjugate 8 in near quantitative yield and in high purity (see ESI† for details). With aza-BODIPY-trastuzumab conjugate 8 in hand, we next appraised its potential as a tool for FGS.

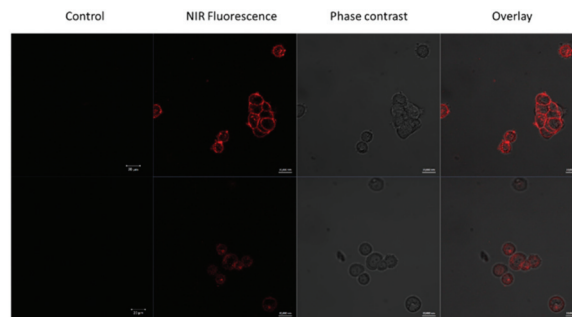


Fig. 3 CLSM images of BT-474 (HER2+) and MDA-MB-468 (HER2-) incubated with 5  $\mu$ M conjugate 8 and control.

### Cell imaging to produce fluorescence imaging

To demonstrate the NIR fluorescence imaging properties of conjugate 8, *in vitro* validation was carried out using cells which overexpress the HER2 cell surface receptor (BT-474), and another cell line which expresses normal levels of the same receptor (MDA-MB-468) (HER2-), using fluorescence microscopy. The two cell lines were individually incubated with 5  $\mu$ M of 8 for 30 min at 4 °C. Excess conjugate was removed by washing with PBS prior to confocal laser scanning microscopy (CLSM) imaging. Fig. 3 shows that, when excited at 633 nm, intense fluorescence predominately localised at the surface of the membrane was observed for BT-474 cells. Fluorescence was confined to the membrane suggesting receptor binding with no non-specific internalisation observed (see ESI† for z-stack data). A low, but detectable, intensity of fluorescence was found for MDA-MB-468 cells. This was expected as these cells express native levels of HER2 receptor, rather than overexpressing it as suggested by Lawrence *et al.*<sup>32</sup> The calculation of the total corrected cellular fluorescence also confirms the significantly higher fluorescence seen for BT-474 cells (see ESI†).

## Conclusions

In conclusion, an aza-BODIPY with enhanced water solubility and NIR emission was synthesised. Regioselective and stoichiometrically-controlled bioconjugation to a clinical relevant antibody (trastuzumab) generated the first targeted aza-BODIPY-antibody conjugate. Validation of cell surface receptor binding using *in vitro* CLSM imaging demonstrated selectivity toward HER2 receptors, highlighting the potentials for aza-BODIPY-antibody conjugates as promising NIR fluorescence probes for *in vivo* imaging with promising applications in FGS.

## Experimental

### Materials and methods

A Jeol JNMLA NMR spectrometer was used to measure <sup>1</sup>H NMR at 400.18 MHz, <sup>19</sup>F NMR at 376.54 MHz and <sup>13</sup>C NMR at



100.62 MHz, the measurement was referenced against standard internal tetramethylsilane (TMS). Splitting patterns were written as s (singlet), d (doublet), t (triplet) and m (multiplet). The chemical shifts ( $\delta$ ) for  $^1\text{H}$ ,  $^{19}\text{F}$  and  $^{13}\text{C}$  are were measured in ppm.

Mass spectrum data was obtained from the National Mass Spectrometry Service EPSRC, Swansea using LTQ Orbitrap XL mass spectrometer. A Varian Cary 50 Bio UV-vis spectrometer was used measuring absorptions from 250 nm to 800 nm. A Varian Cary Eclipse Fluorescence spectrometer was used measuring excitations and emissions from 400 nm to 800 nm.

Reagents were purchased from Alfa Aesar, ACROS Organic, Fluorochem and Sigma Aldrich, and used as received. Dry solvents were obtained through drying over molecular sieves applying the method of Williams *et al.*<sup>33</sup> Rotary evaporation under reduced pressure and a vacuum oven were used to removed excess solvents.

Synthesis of **1** and **5** was carried out in accordance to previously described methodology.<sup>26,31</sup>

### Photostability

Photostability experiments were conducted in a 46 mm  $\times$  12.5 mm  $\times$  12.5 mm quartz cuvette in PBS pH 7.4 solution at 298 K under continuous illumination direct from above the cuvette for 60 min. The NIR light source was a 600 mW Paterson Xenon short arc lamp and equipped with a band pass filter to obtain NIR light 685–733 nm. The intensity of the light from the same distance was measured with Macam R203 Radiometer to be 1709.8 W m<sup>-2</sup>. Measurement was taken every 10 min with a Varian Cary 50 Bio UV-vis spectrometer was used measuring absorptions from 250 nm to 800 nm.

### Fluorescence quantum yield

Five concentrations with normalised absorptions for compound **8** was used for this experiment, and calculated using the equation below:<sup>34</sup>

$$\phi_X = \phi_{ST} \left( \frac{F_X \{1 - \exp(-A_{ST} \ln 10)\}}{F_{ST} \{1 - \exp(-A_X \ln 10)\}} \right) \left( \frac{\eta_X^2}{\eta_{ST}^2} \right)$$

$\phi_X$  is the experimental fluorescence quantum yield of the analyte,  $\phi_{ST}$  is the literature fluorescence quantum yield of the standard,  $F$  is the integrated fluorescence intensity,  $A$  is the absorbance at the excitation wavelength, and  $n$  is the refractive index of the solvent. The two reference systems used were cross-calibrated to obtain fluorescein ( $\phi_f = 0.98$  in 0.1 M NaOH)<sup>35</sup> and rhodamine B ( $\phi_f = 0.30$  in water).<sup>36</sup>

### Synthetic procedures

**tert-Butyl 2-(4-(7-(4-(2-(2-(2-azidoethoxy)ethoxy)ethoxy)phenyl)-5,5-difluoro-1,9-diphenyl-5H-4l4,5l4-dipyrrolo[1,2-c:2',1'-f][1,3,5,2]triazaborinin-3-yl)phenoxy)acetate (2).** A solution aza-BODIPY **1** (80 mg, 0.12 mmol) in dry DMSO (8 mL) was treated with CsF (88 mg, 580 mmol) and *tert*-butylbromoacetate (280 mg, 0.14 mmol). The mixture stirred at 40 °C for 3 h. The mixture was then cooled in an ice bath to 0 °C, a satu-

rated solution of NH<sub>4</sub>Cl (12 mL) was added and the product extracted with ethyl acetate (2  $\times$  50 mL). The combined organic layers were washed with brine, dried over anhydrous Na<sub>2</sub>SO<sub>4</sub>, filtered and the solvent was removed under reduced pressure. The crude was purified by column chromatography on silica gel (50% EtOAc/hexane) and precipitated from hexane over DCM to afford a metallic red solid (72 mg, 78%)  $R_f = 0.51$  (silica, 5 : 5, EtOAc : hexane). UV-vis (DCM):  $\lambda_{\text{max}}$ , nm (log  $\epsilon$ ) 660 (4.98). Fluorescence (DCM):  $\lambda_{\text{max}}$ , (exc/em) nm 660/697.  $^1\text{H-NMR}$  (CDCl<sub>3</sub>):  $\delta$  1.53 (s, 9H, Boc), 3.40 (t,  $J = 4.9$  Hz, 2H, CH<sub>2</sub>N<sub>3</sub>), 3.76–3.63 (m, 4H, PEG), 3.83–3.74 (m, 2H, PEG), 3.94 (t,  $J = 4.8$  Hz, 2H, PEG) 4.24 (t,  $J = 4.9$  Hz, 2H, PEG), 4.61 (s, 2H, CH<sub>2</sub>), 6.93 (s, 2H, Py) 7.00 (dd,  $J = 8.8$ , 6.1 Hz, 4H, *o*-Ar), 7.48–7.46 (m, 6H, *m,p*-Ph), 8.06–8.01 (m, 8H, *o*-Ph, *m*-Ar).  $^{13}\text{C-NMR}$  (CDCl<sub>3</sub>):  $\delta$  28.18 (Boc), 50.78, 65.73, 67.68, 69.87, 70.23, 70.87, 71.04, 82.75, 114.89, 114.94, 125.49, 126.26, 128.61, 129.57, 129.59, 129.64, 130.72, 130.79, 130.95, 131.87, 131.90, 159.18, 160.33, 167.77 (C=O). MS: (APCI)  $m/z$  801 (100 [M + H<sup>+</sup>]), HRMS: 801.3383 calcd for (C<sub>44</sub>H<sub>44</sub>O<sub>6</sub>N<sub>6</sub><sup>10</sup>BF<sub>2</sub>) found 801.3381.

**2-(4-(7-(4-(2-(2-(2-Azidoethoxy)ethoxy)ethoxy)phenyl)-5,5-difluoro-1,9-diphenyl-5H-4l4,5l4-dipyrrolo[1,2-c:2',1'-f][1,3,5,2]triazaborinin-3-yl)phenoxy)acetic acid (3).** A solution of *tert*-butyl 2-(4-(7-(4-(2-(2-(2-azidoethoxy)ethoxy)ethoxy)phenyl)-5,5-difluoro-1,9-diphenyl-5H-4l4,5l4-dipyrrolo[1,2-c:2',1'-f][1,3,5,2]triazaborinin-3-yl)phenoxy)acetate (68 mg, 0.08 mmol) in dry DCM (2 mL) was treated with TFA (0.5 mL), and the mixture stirred at rt for 1.5 h under Ar before the solvent removed under reduced pressure. The residue was purified by column chromatography on silica (DCM to 4% MeOH/DCM) and precipitated from hexane over DCM to yield a metallic red solid (15 mg, 34%).  $R_f = 0.66$  (silica, 10% MeOH : DCM) and 0.29 (silica, KNO<sub>3</sub> : water : MeCN). UV-vis (DCM):  $\lambda_{\text{max}}$ , nm (log  $\epsilon$ ) 660 (4.35). Fluorescence (DCM):  $\lambda_{\text{max}}$ , (exc/em) nm 660/693.  $^1\text{H-NMR}$  (d<sub>6</sub>-DMSO):  $\delta$  3.67–3.61 (m, 8H, PEG), 3.82 (t,  $J = 4.5$  Hz, 2H, PEG), 4.21 (t,  $J = 4.8$  Hz, 2H, PEG), 4.80 (s, 2H, CH<sub>2</sub>), 7.07 (dd,  $J = 6.7$ , 8.8 Hz, 4H, *o*-Ar), 7.56 (s, 1H, Py), 7.57 (s, 1H, Py), 7.69–7.57 (m, 6H, *m,p*-Ph), 8.12–8.00 (m, 8H, *o*-Ph, *m*-Ar).  $^{13}\text{C-NMR}$  (d<sub>6</sub>-DMSO):  $\delta$  50.51, 65.08, 67.82, 69.51, 69.83, 70.25, 70.50, 112.44, 113.46, 115.03, 115.08, 115.13, 115.23, 115.30, 127.25, 127.29, 129.97, 130.56, 130.66, 130.69, 131.21, 155.10, 155.71, 170.71 (C=O).  $^{19}\text{F-NMR}$  (d<sub>6</sub>-DMSO):  $\delta$  -130.83 (q,  $J = 62.5$ , 31.3 Hz). MS: (ESI)  $m/z$  743 (100 [M - H<sup>-</sup>]), HRMS: 742.2643 calcd for (C<sub>40</sub>H<sub>34</sub>O<sub>6</sub>N<sub>6</sub><sup>10</sup>BF<sub>2</sub>) found 742.2633.

**2-(4-(7-(4-(2-(2-(2-Azidoethoxy)ethoxy)ethoxy)phenyl)-5,5-difluoro-1,9-diphenyl-5H-4l4,5l4-dipyrrolo[1,2-c:2',1'-f][1,3,5,2]triazaborinin-3-yl)phenoxy)-N-(2-(2-methoxyethoxy)ethyl)acetamide (4).** 2-(4-(7-(4-(2-(2-(2-Azidoethoxy)ethoxy)ethoxy)phenyl)-5,5-difluoro-1,9-diphenyl-5H-4l4,5l4-dipyrrolo[1,2-c:2',1'-f][1,3,5,2]triazaborinin-3-yl)phenoxy)acetic acid (11 mg, 0.02 mmol), HOBt (11 mg, 0.08 mmol, 5.3 eq.) EDC (11 mg, 0.14 mmol, 9.2 eq.), methoxypolyethylene glycol amine M.W. 5000 (115 mg, 0.02 mmol, 1.5 eq.) and DIPEA (27  $\mu\text{L}$ , 0.31 mmol, 20.5 eq.) were dissolved in dry DMF (2.2 mL) and the reaction mixture stirred overnight at 40 °C. The solvent was





then removed under reduced pressure and further purified by Sep Pak C18 reverse phase cartridge eluting with water and precipitated from DCM over diethyl ether to give the product as a yield a dark blue solid (84 mg, 98%).  $R_f = 0.64$  (silica,  $\text{KNO}_3$ :water:MeCN). UV-vis (water):  $\lambda_{\text{max}}$ , nm ( $\log \epsilon$ ) 635 (4.37). Fluorescence (water):  $\lambda_{\text{max}}$ , (exc/em) nm 635/713.  $^1\text{H-NMR}$  ( $\text{CDCl}_3$ ):  $\delta$  3.93–3.36 (m, PEG 5k), 4.23 (s, 2H,  $\text{CH}_2$ ), 6.91 (s, 1H, Py), 6.93 (s, 1H, Py), 7.05–6.96 (m, 4H, *o*-Ar), 7.52–7.40 (m, 6H, *m,p*-Ph), 8.16–7.91 (m, 8H, *o*-Ph, *m*-Ar).  $^{19}\text{F-NMR}$  ( $\text{CDCl}_3$ )  $\delta$  -130.80 (q,  $J = 61.4, 30.6$  Hz), -130.91 (q,  $J = 62.3, 31.1$  Hz). MS: (MALDI) normal distribution with  $m/z$  5649.1.

### Preparation of conjugate 8

To a solution of trastuzumab (100  $\mu\text{L}$ , 50  $\mu\text{M}$ , 1 eq.) in borate buffer (25 mM sodium borate, 25 mM NaCl, 0.5 mM EDTA, pH 8.0) was added TCEP (final concentration 500  $\mu\text{M}$ , 10 eq.) and 5 in DMSO (final concentration 1.0 mM, 25 eq.) and the reaction mixture incubated at 4  $^\circ\text{C}$  for 16 h. The excess reagents were then removed by repeated diafiltration into fresh buffer using VivaSpin sample concentrators (GE Healthcare, 10 000 MWCO). Following this, analysis by 10% SDS-PAGE gel and UV-Vis revealed conversion to the desired Her-Mestra conjugate with a PD-to-antibody ratio of *ca.* 4. Then, aza-BODIPY 4 (8 eq. from a 20 mM solution in DMSO) was added and the reaction mixture incubated at 21  $^\circ\text{C}$  for 6 h. The resulting mixture was then incubated for 10 minutes with protein A immobilised on beads and washed following manufacturer's protocol. Following this, analysis by SDS-PAGE gel and UV-Vis revealed conversion to the desired Her-Mestra-aza-BODIPY conjugate 8 with a porphyrin-to-antibody ratio of *ca.* 4.

### Conflicts of interest

There are no conflicts to declare.

### Acknowledgements

The authors thank the EPSRC UK National Mass Spectrometry Facility at Swansea University for the acquisition of Mass spectrometry data.

### Notes and references

- J. Rao, A. Dragulescu-Andrasi and H. Yao, *Curr. Opin. Biotechnol.*, 2007, **18**, 17–25.
- A. L. Vahrmeijer, M. Hutteman, J. R. van der Vorst, C. J. H. van de Velde and J. V. Frangioni, *Nat. Rev. Clin. Oncol.*, 2013, **10**, 507–518.
- A. Van Cleef, S. Altintas, M. Huizing, K. Papadimitriou, P. Van Dam and W. Tjalma, *Facts Views Vis Obgyn.*, 2014, **6**, 210–218.
- M. Gao, F. Yu, C. Lv, J. Choo and L. Chen, *Chem. Soc. Rev.*, 2017, **46**, 2237–2271.
- Y. Ni and J. Wu, *Org. Biomol. Chem.*, 2014, **12**, 3774–3791.
- H. Liu, J. Mack, Q. Guo, H. Lu, N. Kobayashi and Z. Shen, *Chem. Commun.*, 2011, **47**, 12092–12094.
- H. C. Daly, G. Sampedro, C. Bon, D. Wu, G. Ismail, R. A. Cahill and D. F. O. Shea, *Eur. J. Med. Chem.*, 2017, **135**, 392–400.
- S. Bhuniya, M. H. Lee, H. M. Jeon, J. H. Han, J. H. Lee, N. Park, S. Maiti, C. Kang and J. S. Kim, *Chem. Commun.*, 2013, **49**, 7141–7143.
- X. Jing, F. Yu and L. Chen, *Chem. Commun.*, 2014, **50**, 14253–14256.
- J. Xu, J. Zhai, Y. Xu, J. Zhu, Y. Qin and D. Jiang, *Analyst*, 2016, **141**, 2380–2383.
- T. Li, T. Meyer, R. Meerheim, H. Marco and K. Christian, *J. Mater. Chem. A*, 2017, **31**, 10696–10703.
- J. Joshi, T. Kumari and Y. Duchaniya, *Int. J. Eng. Technol. Manage. Appl. Sci.*, 2015, **3**, 200–211.
- S. Schutting, T. Jokic, M. Strobl, S. M. Borisov, D. De Beer and I. Klimant, *J. Mater. Chem. C*, 2015, **3**, 5474–5483.
- Y. Ge and D. F. O'Shea, *Chem. Soc. Rev.*, 2016, **45**, 3846–3864.
- D. Wu, S. Cheung, M. Devocelle, L.-J. Zhang, Z.-L. Chen and D. F. O'Shea, *Chem. Commun.*, 2015, **51**, 16667–16670.
- M. Tasior and D. F. O. Shea, *Bioconjugate Chem.*, 2010, **21**, 1130–1133.
- A. Loudet, R. Bandichhor, L. Wu and K. Burgess, *Tetrahedron*, 2008, **64**, 3642–3654.
- G. J. Weiner, *Nat. Rev. Cancer*, 2015, **15**, 361–370.
- X. Zhang, G. Soori, T. J. Dobleman and G. G. Xiao, *Expert Rev. Mol. Diagn.*, 2014, **14**, 97–106.
- J. M. Warram, E. de Boer, M. Korb, Y. Hartman, J. Kovar, J. M. Markert, G. Y. Gillespie and E. L. Rosenthal, *Br. J. Neurosurg.*, 2015, **8697**, 1–9.
- K. E. Day, L. N. Beck, C. H. Heath, C. C. Huang, K. R. Zinn and E. L. Rosenthal, *Cancer Biol. Ther.*, 2013, **14**, 271–277.
- J. McMahon, C. J. O. Brien, I. Pathak, R. Hamill, E. Mcneil and N. Hammersley, *Br. J. Oral Maxillofac. Surg.*, 2003, **41**, 224–231.
- J. M. Warram, E. De Boer, G. M. Van Dam, L. S. Moore, S. L. Bevans, E. M. Walsh, E. S. Young, W. R. Carroll, T. M. Stevens and E. L. Rosenthal, *J. Pathol.: Clin. Res.*, 2016, **2**, 104–112.
- T. Barrett, Y. Koyama, Y. Hama, G. Ravizzini, I. S. Shin, B. Jang, C. H. Paik, Y. Urano, P. L. Choyke and H. Kobayashi, *Clin. Cancer Res.*, 2007, **13**, 6639–6649.
- A. Maruani, M. E. B. Smith, E. Miranda, K. A. Chester, V. Chudasama and S. Caddick, *Nat. Commun.*, 2015, **6**, 6645–6654.
- A. Maruani, H. Savoie, F. Bryden, S. Caddick, R. Boyle and V. Chudasama, *Chem. Commun.*, 2015, **51**, 15304–15307.
- M. T. W. Lee, A. Maruani, J. R. Baker, S. Caddick and V. Chudasama, *Chem. Sci.*, 2016, **7**, 799–802.
- V. Chudasama, A. Maruani and S. Caddick, *Nat. Chem.*, 2016, **8**, 114–119.



- 29 M. T. W. Lee, A. Maruani, D. A. Richards, J. R. Baker, S. Caddick and V. Chudasama, *Chem. Sci.*, 2017, **8**, 2056–2060.
- 30 E. Robinson, J. P. M. Nunes, V. Vassileva, A. Maruani, J. C. F. Nogueira, M. E. B. Smith, R. B. Pedley, S. Caddick, J. R. Baker and V. Chudasama, *RSC Adv.*, 2017, **7**, 9073–9077.
- 31 M. H. Y. Cheng, H. Savoie, F. Bryden and R. W. Boyle, *Photochem. Photobiol. Sci.*, 2017, **16**, 1260–1267.
- 32 R. T. Lawrence, E. M. Perez, C. A. Blau, C. P. Miller, K. M. Haas, H. Y. Irie, R. T. Lawrence, E. M. Perez and D. Herna, *Cell Rep.*, 2015, **11**, 630–644.
- 33 D. B. G. Williams and M. Lawton, *J. Org. Chem.*, 2010, **75**, 8351–8354.
- 34 A. M. Brouwer, *Pure Appl. Chem.*, 2011, **83**, 2213–2228.
- 35 J. R. Lakowicz, *Principles of Fluorescence Spectroscopy*, Kluwer Academic/Plenum Publishers, 2nd edn, 1999.
- 36 D. Magde, G. E. Rojas and P. G. Seybold, *Photochem. Photobiol.*, 1999, **70**, 737–744.

